組織再生材料(TEC)/コラーゲンシート複合体の引張特性

首都大学東京大学院システムデザイン研究科
池谷　基志・藤江　裕道

東海大学工学部機械工学科
大家　　渓

札幌医科大学生体工学・運動器治療開発講座
鈴木　大輔

株式会社ニッピ　バイオマトリックス研究所
小倉　孝之・小山　洋一

大阪大学整形外科
杉田　憲彦・中村　憲正

臨床バイオメカニクス, Vol. 35, 2014.

臨床バイオメカニクス，Vol. 35，2014.

組織再生材料(TEC)/コラーゲンシート複合体の引張特性

池谷　基志[※1]　大家　渓[※2]　鈴木　大輔[※3]　小倉　孝之[※4]
小山　洋一[※4]　杉田　憲彦[※5]　中村　憲正[※5]　藤江　裕道[※1]

Tensile properties of stem cell-based tissue engineered construct (TEC) cultured on a collagen sheet.

Motoshi IKEYA, B.S., Kei OYA, Ph.D., Daisuke SUZUKI, Ph.D.,
Takayuki OGURA, Youichi KOYAMA, Norihiko SUGITA, M.D., Ph.D.,
Norimasa NAKAMURA, M.D., Ph.D., Hiromichi FUJIE, Ph.D.

Abstract

We have been developing a novel tissue-engineering technique for the repair of cartilage, ligaments, and tendons, which involves a stem cell-based tissue engineered construct (TEC). However, cartilage-like tissues repaired with pure TEC are inferior to normal cartilage in terms of permeability, compressive properties, and friction properties. To solve these problems, we developed TEC combined with a collagen sheet (CS) in the present study. Mesenchymal stem cells (MSCs) were obtained from synovial membranes of a human knee joint. The cells were plated to develop TEC on the CS for 7, 14, and 28 days. Scanning electron microscopy indicated that there are more MSC in the upper layer of TEC on CS at 28 days. The tangent modulus and strength of TEC significantly increased over the culture period, and were higher than those of CS soaked in culture medium at 28 days.

Key words : Stem cell-based tissue engineered construct (TEC), Tissue engineering, Collagen sheet, Tensile property.

※ 1　首都大学東京大学院システムデザイン研究科　〒191-0065　東京都日野市旭ヶ丘6-6
※ 2　東海大学工学部機械工学科　〒259-1292　神奈川県平塚市北金目4-1-1
※ 3　札幌医科大学生体工学・運動器治療開発講座　〒060-0061　北海道札幌市中央区南1条西17
※ 4　株式会社ニッピ　バイオマトリックス研究所　〒302-0017　茨城県取手市桑原520-11
※ 5　大阪大学整形外科　〒565-0871　大阪府吹田市山田丘2-2

Corresponding Author : Hiromichi FUJIE, PhD. Faculty of System Design, Tokyo Metropolitan University.
6-6 Asahigaoka, Hino, Tokyo, 191-0065, Japan.
Tel & Fax : 042-585-8628　E-mail address : fujie@sd.tmu.ac.jp

緒　　言

我々は損傷した軟骨，腱，靱帯を修復することを目的に，幹細胞を含む自己生成組織であるTEC（stem cell-based tissue engineered construct)[1] に関する研究を行っている．TECは，細胞と細胞自身が産生する細胞外基質（タイプⅠ，Ⅲコラーゲン，フィブロネクチン，ヴィトロネクチン）からなる組織であり，動物由来のコラーゲンや人工化合物からなるスキャフォールドを必要としないため，生体内に埋入した際に拒否反応等を起こしにくいといった特徴を有している．TECはすでに軟骨修復において優れた効果があることがわかっている[1]が，TECによる修復軟骨の力学特性は正常と比較して劣っており，特にコラーゲン密度が高い軟骨表層の修復が課題となっている[6]．一方，腱，靭帯修復のための研究もこれまで行われてきたが，TECのコラーゲン密度が低く，強度が不足しているために実用化には至っていない[9)~11]．そこで，TECとコラーゲンシート（CS）を複合させることで，TECのコラーゲン密度を増大させることを考案した．CSはブタ真皮由来のコラーゲン線維からなるシートであり，線維組織の修復に効果があることが報告されている[12]．また，コラーゲンは細胞の伸展，増殖や細胞外基質生成を促進させることが知られており[3),4]，CSとTECを複合させることで，軟骨最表層や腱，靭帯修復において優れた効果が期待できる．本研究では，CSを培養基板として用いてTEC/CS複合体を作製し，TEC/CS複合体の組織観察および引張試験を行い，その構造と引張特性について調べた．

実験方法

1．CSの作製

ブタ真皮由来ペプシン可溶化コラーゲン（3 mg/mL）に対して，等量の二倍濃縮PBS（−）溶液を加え撹拌した後，37℃で24時間インキュベートすることで，再構成線維を得た．得られた線維を，ホモジナイザーにて破砕し，遠心分離機にて回収した．沈殿物にエタノールを加え，ミキサーを用いて細かく分散後，この分散体を孔径1 μmのフィルターで濾取し，シート状の線維堆積物を得る．エタノールを自然乾燥させることでCSを作製した．このCSは生体組織と同様の20～30%程度のコラーゲン密度，多孔性，架橋剤を用いていないといった特徴を有している[12]．

2．TEC/CS複合体の作製

CSを組織培養皿上に設置しコラーゲンゲルを用いて固定した．その後，ヒト膝関節滑膜より採取した幹細胞を含む滑膜由来細胞を，5回の継代培養の後，初期細胞密度4.0×10^5 cells/cm^{2}で培養培地（DMEM，10%ウシ胎児血清，ペニシリン（100 U/mL）/ストレイプトマイシン（100 μg/mL））中に播種した．細胞外基質生成を促進させるためアスコルビン酸2リン酸を0.2mM添加した[2),9)]．7，14，28日間培養を行いTEC/CS複合体を作製した．組織培養皿上を用いて同様の条件で滑膜由来細胞を28日間培養し，培養皿底面に生成した基質と細胞を剥離して1時間自己収縮させることでTECを生成した（TEC 28d群）．また，培地に28日間浸漬したCS（CS 28d群）と培地に浸漬していないCS（CS 0d群）を比較対照として用いた．

3．組織観察

TEC/CS 7d，28d群をKarnovsky溶液[7]で前固定した後，1%四酸化オスミウム溶液により後固定処理を行った．その後，50，70，80，90，95，100%の順にエタノールで脱水し，臨界点乾燥した．Pt-Pdを10 nmコーティングした後，走査型電子顕微鏡（JSM-6380LA，JEOL）で観察した．また，Karnovsky溶液により固

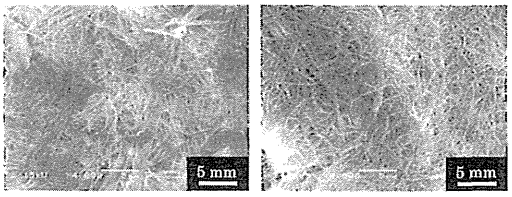

CS 0d　　CS 28d

図1．Microscopic observation of collagen sheet soaked in culture medium for 0 and 28 days.

定処理を行った後，70，80，90，100％のエタノールで順に脱水し，キシレンで置換後にパラフィンに浸漬し，パラフィンブロックを作製した．ミクロトーム（REM-710，大和工機工業）を用いて厚さ4 μmに切り出し，ヘマトキシリンで核を，エオジンで細胞質類を染色し（HE染色），組織の断面を観察した．

4．引張試験

試験片をスライドガラスに広げてPBS（-）溶液を10 μL添加し，カバーガラスで挟みデジタルマイクロスコープ（VHX-100，KEYENCE）を用いて，スライドガラスとカバーガラス間距離を5カ所測定し，測定した値の平均を厚さとした．

試験片の引張特性解析のため，齊藤らが作製した引張試験機[10]を用いた（図2）．各群をリニアアクチュエータ（LAH-46-3002-F-PA，ハーモニックドライブシステムズ）側と荷重検出側に接続したチャック部に挟み込み，幅が6 mmになるよう両側を切り揃えた．リニアアクチュエータを用いて，プレロードを2 mN与えた後に，引張速度0.05 mm/sで試験片が破断するまで荷重を与えた．引張荷重は2枚のひずみゲージ（KFG-02-120-C1-23，KYOWA）を貼った板バネ状の荷重センサで計測した．ひずみは，試験片の固定両端から6 mm以上離れた2点において，微小磁石（重量0.002 g，寸法1×1×1 mm）と発泡スチロールビーズ（Φ2 mm）を用いて作製したマーカを試験片の上下から挟み，この2点間距離の変化をCCDカメラ（CV-070，KEYENCE）と画像センサ（CV-750，KEYENCE）で追跡して非接触で求めた．シリコンラバーヒータ（一般用SR，スリーハイ）と温度コントローラ（ON-DO2，ワンダーキット）を用いて，37℃に保たれたPBS（-）溶液中で試験を行った．厚さと引張試験機のチャック幅6 mmから断面積を求め，荷重と断面積より公称応力を求めた．また応力－ひずみ線図の線形部分における接線係数を求めた．

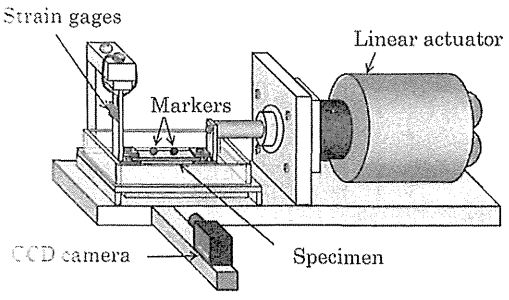

図2．Schematic image of the tensile test system for TEC/CS.

結　　果

1．組織観察結果

組織断面のSEM像とHE染色像の観察結果から，TEC/CS 7d群では，組織表面に多くの細胞が観察されたのに対し，TEC/CS 28d群は組織表面から約100 μmの深さまでコラーゲンの分解が進み，より多くの細胞がコラーゲンシート内に侵入していた（図3）．

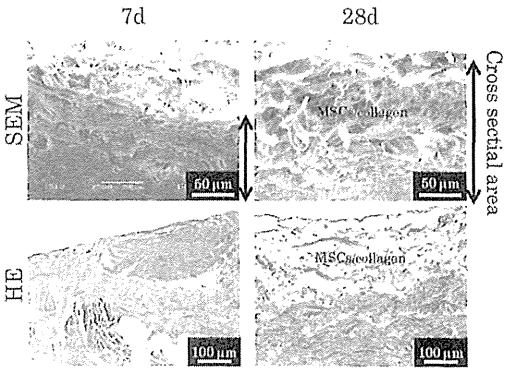

図3．Optical microscopic (HE stain) and scanning electron microscopic observation of the cross-sectional area of the TEC/CS.

2．厚さ測定結果

厚さ測定の結果，CS 0d群は331.0±29.0 μm，CS 28d群は931.3±122.8 μm，TEC 28d群は288.3±75.6 μm，TEC/CS 7d群は1319.6±137.9 μm，TEC/CS 14d群は891.6±65.7 μm，TEC/CS 28d群は854.5±87.2 μmとなった．CS 0d群と比較してTEC/CS群，CS28d群の厚さは有意に増大した．TECをCSと複合させて一週間培養したTEC/CS 7d群はCS 28d群と比較して厚さが有意に増大したが，二週間および四週間培養したTEC/CS 14d，28d群では厚さ

が有意に減少した．

3．引張試験結果

CS 0d群の破断強度は274.9±80.1 kPa，接線係数は1093.9±617.6 kPaであったが，浸漬28日後のCS 28d群の破断強度は13.6±5.0 kPa，接線係数は52.1±15.0 kPaとなり有意に低下した．また，CSを用いないで培養したscSAT 28d群の破断強度は66.2±27.9 kPa，接線係数は515.9±194.2 kPaだった．これらに対し，TECとCSを複合させて7日間培養したTEC/CS 7d群の破断強度は5.3±1.9 kPa，接線係数は38.4±26.5 kPaだった．14日間培養したTEC/CS 14d群の破断強度は13.9±3.8 kPa，接線係数は73.5±40.2 kPaとなりTEC/CS 7d群と比較して有意に高い値を示し，CS 28d群と同程度の値だった．28日間培養したTEC/CS 28d群の破断強度は15.5±3.9 kPa，接線係数は93.9±52.7 kPaであり，CS 28d群に比べ高い傾向を示し，TEC/CS 7d群と比較して有意に高い値を示した．しかし，TEC 28d群の破断強度，接線係数に比べると有意に低かった．

考　　察

TEC/CS複合体を一週間培養したTEC/CS 7d群の破断強度，接線係数はCS 28d群と比較して減少したが，さらに一週間培養したTEC/CS 14d群の破断強度，接線係数は，TEC/CS 7d群と比較して有意に増加した．四週間培養を継続したTEC/CS 28d群では，さらに破断強度，接線係数が増加した．組織観察結果から考察すると，培養過程でMSCsがCS内部に侵入し，CSのコラーゲンを分解して新たな基質を生成したためと考えられる．この際に，低分子化したコラーゲンペプチドやアスコルビン酸2リン酸などの効果によりMSCsが強固なコラーゲンを生成した可能性も考えられる[8),9)]．本研究結果からTEC/CS複合体は豊富なコラーゲンを含有するとともに，培養を継続することで組織の引張特性向上が可能であることが示された．TECを用いた軟骨修復では，表層のコラーゲン密度が少ないため透水率が高い値となり，

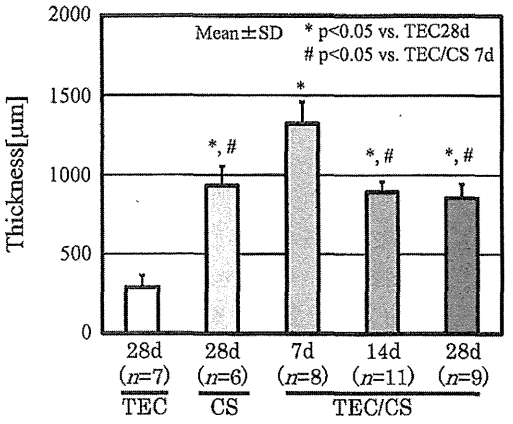

図4．Thickness of the TEC 28d, CS 28d, TEC/CS 7d, 14d, 28d groups.

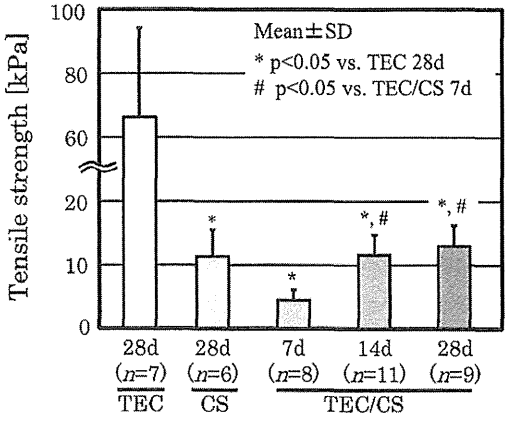

図5．Tensile strength of the TEC 28d, CS 28d, TEC/CS 7d, 14d, 28d groups.

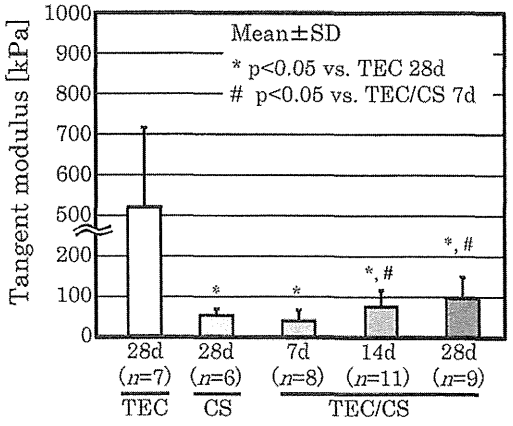

図6．Tangent modulus of the TEC 28d, CS 28d, TEC/CS 7d, 14d, 28d groups.

圧縮特性や摩擦特性が正常軟骨レベルまで回復しないという問題が指摘されている[5]．本研究で開発したTECとCSの複合体により，この問題を解決できる可能性がある．

一方，CSを用いずに生成したTEC 28d群と比較して，TEC/CS 28d群の破断強度，接線係数は有意に低い値を示し，組織の強度がより重要になる腱，靭帯の修復に応用は困難であると考えられる．TEC/CS複合体の強度が低下した原因に，培地に浸漬したことによるCSの強度低下が考えらえる．四週間培養したTEC/CS 28d群の組織観察ではCS上層部にのみMSCsが存在していた．CS内に均等にMSCsを浸潤させ，CSのコラーゲンの分解と細胞外基質の生成を促すことで組織の高強度化が可能であると考えられる．

結　　言

CSを培養基板としてTECを作製することで，TEC/CS複合体を作製し．組織観察と引張試験を行った．その結果．7日間培養したTEC/CS複合体は28日間培地に浸漬したCSと比較して強度が低下したが．TEC/CS複合体を28日間培養することでより多くの細胞がCS内部に侵入し，強度が向上することがわかった．

＜謝　　辞＞

この研究は，科研費基盤研究B（25282134），首都大学東京全学傾斜研究費（医工連携），文部科学省私立大学戦略的研究基盤形成支援事業「工学院大総研FMS」の助成を受けた．

文　　献

1）Ando W., Tateishi K., et al. : Cartilage repair using an in vitro generated scaffold-free tissue-engineered construct derived from porcine synovial mesenchymal stem cells. Biomaterials : 28, 5423-5470, 2007.

2）Ando W., Nakamura N., et al. : In vitro generation of a scaffold-free tissue-engineered construct (TEC) derived from human synovial mesenchymal stem cells, biological and mechanical properties and further chondrogenic potential, Tissue Engineering : 14, 2041-2049, 2008.

3）Eileen G., Kay C. Dee, et al. : Mechanical characterization of collagen fibers and scaffolds for tissue engineering, Biomaterials : 24, 3805-3813, 2003.

4）Huang D., Ehrlich HP., et al. : Mechanisms and dynamics of mechanical strengthening in ligament-equivalent fibroblast-populated collagen matrices, Ann Biomed Eng : 21, 289-305, 1993.

5）今出久一郎，藤江裕道，他：膝関節軟骨表層の透水率が摩擦特性に及ぼす影響，臨床バイオメカニクス：34，441-445，2013.

6）井村眞知子，藤江裕道，他：滑膜由来間質細胞から生成した組織再生材料（TEC）の軟骨修復への応用，日本臨床バイオメカニクス学会誌：29，135-140，2008.

7）Karnovsky M. J. : A formaldehyde glutaraldehyde fixative of high osmolarity for use in electron microscopy, J. Cell Biol : 27, 137A-138A, 1965.

8）Matsuda N., Takehana K., et al. : Effects of ingestion of collagen Fibrils and glycosaminoglycans in the Dermis, J Nutr Sci Vitaminol, 52, 211-215, 2006.

9）永井清人，藤江裕道，他：滑膜由来間質細胞から生成したスキャフォールドフリー三次元人工組織の力学特性，日本臨床バイオメカニクス学会誌：27，89-93，2006.

10）齊藤佳，藤江裕道，他：滑膜由来幹細胞自己生成組織の引張荷重下による強度向上，臨床バイオメカニクス学会誌：30，1-4，2009.

11）須玉裕貴，藤江裕道，他：マイクロパターン加工培養皿による幹細胞自己生成組織（scSAT）の異方性付与，臨床バイオメカニクス：31，7-12，2010.

12）鈴木大輔，藤宮峯子，他：コラーゲンシートとコラーゲンペプチドを用いた膝蓋靭帯の再生，日本臨床バイオメカニクス学会抄録集：39，161，2012.

ナノ周期構造上で作製した幹細胞自己生成組織（scSAT）の引張特性

首都大学東京大学院システムデザイン研究科
谷　優樹・藤江　裕道

東海大学工学部機械工学科
大家　渓

大阪大学整形外科
杉田　憲彦・中村　憲正

臨床バイオメカニクス，Vol. 35，2014.

ナノ周期構造上で作製した幹細胞自己生成組織（scSAT）の引張特性

谷　優樹[※1]　大家　渓[※2]　杉田　憲彦[※3]　中村　憲正[※3]　藤江　裕道[※1]

Tensile property of stem cell-based self-assembled tissues cultured on a nanoperiodic structured surface.

Yuki TANI, BS., Kei OYA, PhD., Norihiko SUGITA, MD., PhD.,
Norimasa NAKAMURA, MD., PhD., Hiromichi FUJIE, PhD.

Abstract

Stem cell-based self-assembled tissue (scSAT) biosynthesized from synovium-derived mesenchymal stem cells has great potential for the repair and regeneration of biological soft tissues. However, the mechanical properties of scSAT were insufficient for clinical applications. Moreover, the structural and mechanical properties of scSAT are isotropic, while those of ligaments and tendons are anisotropic. A candidate solution to the problem is to promote the generation of the extracellular matrix in scSAT using a special culture on a nano-structured surface. As described above, previous studies indicated that a material having a certain roughness promotes cell adhesiveness and that a material having a nanoperiodic structure enhances the anisotropic property of cells. Therefore, a nanoperiodic structure was processed on a titanium surface using a femtosecond laser system, and the mechanical strength of scSAT cultured on the processed surface was determined in the present study. The tensile strength was significantly higher in scSAT cultured on Nano-Ti than in that on Ti. Microscopic observation indicated that scSAT cultured on Nano-Ti had a nanoperiodic, anisotropic structure. In summary, the tensile strength of scSAT cultured on Ti having a nanoperiodic-structured surface was higher than that cultured on normal Ti.

Key words : Stem cell-based self-assembled tissue (scSAT), Tissue engineering, Tensile property, Anisotropic property.

※ 1　首都大学東京大学院システムデザイン研究科　〒191-0065　東京都日野市旭ヶ丘6-6
※ 2　東海大学工学部機械工学科　〒259-1292　神奈川県平塚市北金目4-1-1
※ 3　大阪大学整形外科　〒565-0871　大阪府吹田市山田丘2-2

Corresponding Author : Hiromichi FUJIE, PhD. Faculty of System Design, Tokyo Metropolitan University.
6-6 Asahigaoka, Hino, Tokyo, 192-0065, Japan.
Tel & Fax : 042-585-8628　E-mail address : fujie@sd.tmu.ac.jp

緒　　言

ヒト膝滑膜から採取した間葉系幹細胞（Mesenchymal stem cells：MSCs）に細胞外基質を自己生成させて作製される組織（Stem cell-based self-assembled tissue：scSAT）[1]が腱や靭帯の新たな再生医療材料として期待されている．しかし，現状のscSATは腱や靭帯の修復のためには力学強度が不足している．この解決策として，MSCsによる細胞外基質の生成を促進させて組織の強度を向上させることと，組織に腱や靭帯のような構造異方性を付与し，一方向への強度を高めることの二つの方法が考えられる．この二つを同時に実現するためには，周期的な溝構造をもつ基板表面上でscSATを作製することが有効である．これまでに，フェムト秒レーザによりチタン表面に形成したナノ周期構造上でMSCsを培養することにより，細胞の接着特性が向上し，細胞配向を制御できることがわかっている[6]．そこで本研究では，フェムト秒レーザによりナノ周期構造を付与したチタン表面上でscSATを作製し，組織の高強度化を図った．

実験方法

1．ナノ周期構造の形成

研磨紙320，600，800，1000番の順で湿式研磨を施した直径19mm，厚さ1.0mmのJIS2種の工業用純チタンを試料とした．基本波長780nmのフェムト秒レーザ装置（IFRIT，サイバーレーザ）を用いて，パルス時間幅190fs，レーザフルエンス0.5J/cm^2，走査速度1200mm/minの条件で作製した（Nano-Ti）．試料表面を走査型電子顕微鏡（SEM，JSM-6380LA，日本電子）により観察し，画像解析ソフト（ImageJ，version 1.46，National Institutes of Health）を用いて，得られたSEM像からナノ周期構造のピッチを測定した．さらに，原子間力顕微鏡（AFM），（VN-8000，キーエンス）を用いて表面形状を計測し，溝の深さと表面粗さ（R_a，R_y，R_z）を測定した．なお，溝のピッチは隣り合う山の頂点間の距離と定義した．

2．試験片

ヒト膝関節滑膜より採取した幹細胞を含む滑膜由来細胞を，6回の継代培養の後，初期細胞密度4.0×10^{5}cells/cm^{2}で培地DMEM（FBS10%，100U/ml Penicillin＋100μg/ml Streptomycin）に播種した．細胞外基質生成を促進させるため，アスコルビン酸2リン酸を0.2mM添加し[2),5)]，14，28日間培養を行った．培養後に培養皿底面に生成した基質と細胞を剥離して1時間自己収縮（静置培養）させることで，組織の厚さを増大させてscSATを作製した（図1）．この時，培養面が平滑なポリスチレン製組織培養皿で作製した試験片をPS群，研磨のみを行ったTi上で作製した試験片をTi群，Nano-Ti上で作製した試験片をNano-Ti群とした．なお，本研究におけるヒト膝滑膜の採取および細胞培養は，大阪大学医学部および工学院大学の倫理審査委員会より承認を得ており，被験者の同意を得た上

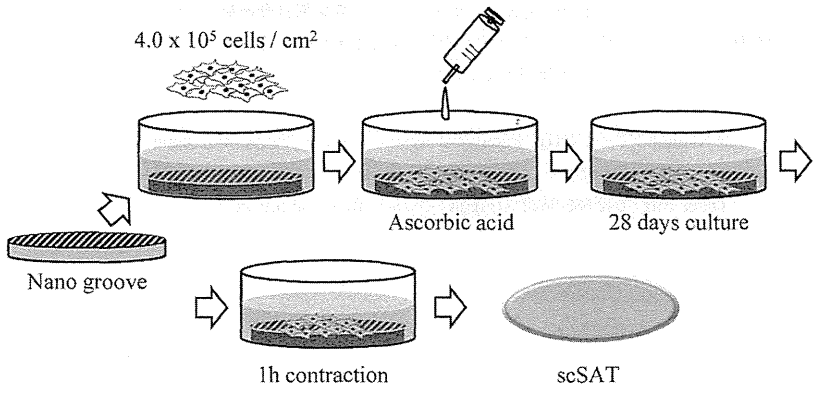

図1．Production procedure of scSAT.

で滑膜の提供を受けている．さらに，本研究はヘルシンキ宣言に則って遂行していることを付記する．

3．組織観察

14日後の各試験片に対して4％パラホルムアルデヒド溶液により固定処理を行い，その後シリウスレッド溶液で組織のコラーゲン線維を赤色に染色し，組織の表面をデジタルマイクロスコープ（VHX-100，KEYENCE）を用いて観察した[7]．培養14日後におけるPS群とNano-Ti群の組織観察を行った．

4．厚さ測定

28日後の各試験片に対して，試験片をスライドガラスに広げてPBS(-)溶液を10μl添加し，その上にカバーガラスで挟んだ．そして，デジタルマイクロスコープ（VHX-100，KEYENCE）を用いて，スライドガラスとカバーガラス間距離を任意の5カ所測定した．測定した値の平均を厚さとし，厚さと引張試験機のチャック幅6 mmから断面積を求め，荷重と断面積より公称応力を求めた[5]．

5．引張試験

試験片の引張特性解析のため，齊藤らが作製した引張試験機[8]を用いた（図2）．試験片は培養皿の溝方向と引張荷重を与える方向が同じになるように，リニアアクチュエータ（LAH-46-3002-F-PA，ハーモニックドライブシステムズ）側と荷重検出側に接続したチャック部に挟み込み，幅が6 mmになるよう両側を切り揃えた．リニアアクチュエータを用いて，プレロードを2 mN与えた後に，引張速度0.05mm/sで試験片が破断するまで荷重を与えた．引張荷重は2枚のひずみゲージ（KFG-02-120-C1-23，KYOWA）を貼った板バネ状の荷重センサで計測した．また，試験環境を生体に模擬するため，シリコンラバーヒータ（一般用SR，スリーハイ）と温度コントローラ（ON-DO2，ワンダーキット）を用いて，37℃に保たれたPBS(-)溶液中で試験を行った．28日間培養したPS群，Ti群，およびNano-Ti群の溝方向に対する引張試験を行った．

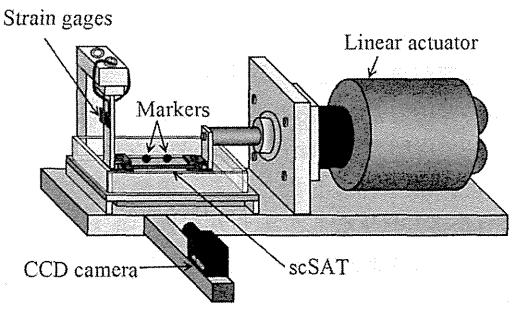

図2．Schematic image of tensile test system.

6．統計解析手法

nを測定回数として，全てのデータは平均±標準偏差（Mean±SD）で表した．2群の場合は2標本t検定で評価した．有意水準はそれぞれ$p<0.05$とした．

結　　果

1．ナノ周期構造の形成

図3にTiとNano-TiのSEM像を示す．Nano-Tiでは，フェムト秒レーザ処理により，ナノ周期構造が形成されていることが確認された．AFMにより表面形状を測定した結果，Nano-Tiのピッチは(540±54nm)（平均±標準偏差），深さは（55.0±23nm），粗さは，R_aが27.0±4.0 nm，R_yが164±13nm，R_zが102±23nmであった．TiのR_a，R_y，R_zはそれぞれ6.20±1.1nm，49.0±10nm，19.0±4.0nmであり，全てのパラメータにおいてNano-Tiの粗さは4倍以上に増大した．

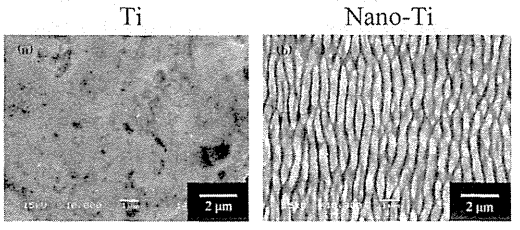

図3．Scanning electron microscope images of Ti (a) and Nano-Ti (b).

2．組織観察結果

デジタルマイクロスコープによる組織観察結果をそれぞれ図4に示す．Nano-Ti群はPS群と比較して濃い染色部分が多く観察された．

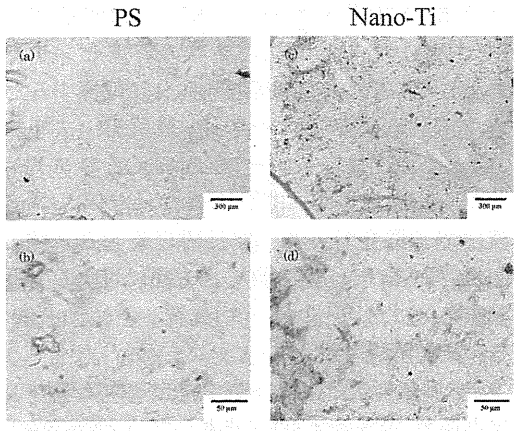

図4．Digital microscopic images of the PS (a) (b) and Nano-Ti (c) (d).

3．厚さ測定結果

PS群の厚さは212±2.0μm，Ti群は173±34μm，Nano-Ti群は206±51μmとなり，PS群およびNano-Ti群ともにTi群と比較して高い傾向を示したが，両者の間に統計的な有意差はなかった．またPS群とNanoi-Ti群との間においても統計的な有意差はなかった．

4．引張試験結果

引張試験より取得した引張強度を図5に示す．Ti群は0.006±0.006MPa，Nano-Ti群は0.045±0.011MPa，PS群は0.060±0.034MPaとなった．Ti群と比較してPS群は有意（p＝0.009）に高い値を示した．また，Ti群と比較してNano-Ti群は引張強度が約7倍に増大し，両群に統計的な有意差（p＝0.03）が見られた．一方，Nano-Ti群とPS群の引張強度に有意差はなかった．

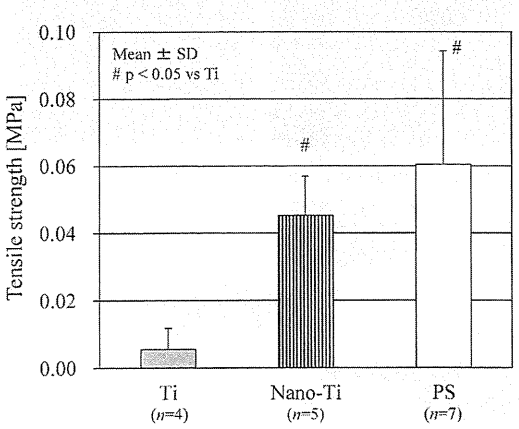

図5．Tensile strength of scSATs produced on Ti, Nano-Ti and PS.

考　　察

組織観察の結果，Nano-Ti群はPS群と比較してコラーゲン線維が濃く染まっていたことから，コラーゲンの産生が促進されていると考えられた．Dongwooらは，粗さ0.645から13.4nmまでの凹凸構造を付与したチタン表面上で骨髄由来MSCsを培養した．結果，細胞から産生されるコラーゲン基質の産生量は最も粗い13.4nmの時に高い値を示したことを報告している[3]．このことから，細胞から産生されるコラーゲン基質量はチタン表面の粗さに依存し，粗い表面であるほど産生されると結論付けた．本研究では，フェムト秒レーザにより加工したチタン表面は未処理のチタンと比較して粗い表面となった．よって，scSATから産生される細胞外基質量は，培養過程におけるナノ周期構造の影響を受け，粗い表面であるほどコラーゲン産生量が増大していることが考えられる．

引張試験において，Ti群がPS群に劣る結果が得られた．Tiは，生体親和性に優れる材料であるが，PSに比べて何らかの悪影響をscSAT生成に及ぼしている可能性がある．チタン表面に構成するナノ周期構造をPDMS（ジメチルポリシロキサン）に転写し，それを培養皿として用いることによりこの問題を解決する必要がある．しかし，Nano-Ti群は材質的には同じTi群と比較して引張強度が有意に高い値を示しており，このことからナノ構造付与により強度が向上したことが理解できる．須玉らは半導体製造で用いられるマイクロ加工技術を導入して作製されたマイクロパターン加工培養皿でscSATを作製したところ，培養皿で培養したscSATと比較して細胞と組織が配向してより強い構造異方性を示すと同時に，配向方向の引張強度が有意に増大することを示した[4),9)]．本研究の結果より，マイクロレベルだけでなく，

ナノレベルの溝構造上でも力学特性に優れたscSATが生成できることがわかった．ただし，マイクロレベルとナノレベルの溝構造では幹細胞の接触様式や，接触による細胞の反応，動態が異なると予想される．この点について今後検討していかなければならない．

結　　言

フェムト秒レーザによりチタン表面に形成したナノ周期構造上で培養を行うことにより，幹細胞自己生成組織（scSAT）を生成した．その結果，未処理のチタン上で作製したscSATと比較して，引張強度が増大し，高強度の組織が作製できることが明らかになった．

＜謝　　辞＞

本研究を行うにあたり，科学研究費助成事業（基盤研究B，25282134），首都大学東京全学傾斜研究費（医工連携），および私立大学戦略的研究拠点形成支援事業（FMS，工学院大学）の支援を受けた．謝意を表する．

文　　献

1）Ando W., Tateishi K., et al. : Cartilage repair using an in vitro generated scaffold-free tissue-engineered construct derived from porcine synovial mesenchymal stem cells. Biomaterials : 28, 5462-5470, 2007.

2）Ando W., Nakamura N., et al. : In vitro generation of a scaffold-free tissue-engineered construct (TEC) derived from human synovial mesenchymal stem cells, biological and mechanical properties and further chondrogenic potential. Tissue Engineering : 14, 2041-2049, 2008.

3）Dongwoo K., Jin-Woo P., et al. : Role of subnano-, nano- and submicron-surface features on osteoblast differentiation of bone marrow mesenchymal stem cells. Biomaterials : 33, 5997-6007, 2012.

4）熊谷賢一，藤江裕道 他：滑膜由来スキャフォールドフリー三次元人工組織の細胞外基質生成能におよぼす力学刺激の影響，日本臨床バイオメカニクス学会誌：28，47－51，2007.

5）永井清人，藤江裕道 他：滑膜由来間質細胞から生成したスキャフォールドフリー三次元人工組織の力学特性，日本臨床バイオメカニクス学会誌：27，89－93，2006.

6）Oya K., Aoki S., et al. : Morphological Observations of Mesenchymal Stem Cell Adhesion to a Nanoperiodic-Structured Titanium Surface Patterned Using Femtosecond Laser Processing : Jpn. J. Appl. Phys. 51, 125203, 2012.

7）Sabine F., Xin J., et al. : Dynamic processes involved in the pre-vascularization of silk fibroin constructs for bone regeneration using outgrowth endothelial cells. Biomaterials : 30 1329-1338, 2009.

8）齊藤佳，藤江裕道 他：滑膜由来幹細胞自己生成組織の引張荷重下による強度向上，臨床バイオメカニクス：30，1－4，2009.

9）須玉裕貴，藤江裕道 他：マイクロパターン加工培養皿による幹細胞自己生成組織（scSAT）の異方性付与，臨床バイオメカニクス：31，7－12，2010.

Biochemical and Biophysical Research Communications 454 (2014) 12–18

Contents lists available at ScienceDirect

Biochemical and Biophysical Research Communications

journal homepage: www.elsevier.com/locate/ybbrc

Cyp26b1 within the growth plate regulates bone growth in juvenile mice

Yoshiki Minegishi [a,b,c], Yasuo Sakai [c,d], Yasuhito Yahara [a], Haruhiko Akiyama [e], Hideki Yoshikawa [f], Ko Hosokawa [c], Noriyuki Tsumaki [a,g,*]

[a] Department of Cell Growth and Differentiation, Center for iPS Cell Research and Application, Kyoto University, 53 Kawahara-cho, Shogoin, Sakyo-ku, Kyoto 606-8507, Japan
[b] Department of Plastic and Reconstructive Surgery, University of Fukui Hospital, 23-3 Matsuokashimoaizuki, Eiheiji-cho, Yoshida-gun, Fukui 910-1193, Japan
[c] Department of Plastic Surgery, Osaka University Graduate School of Medicine, 2-2 Yamadaoka, Suita, Osaka 565-0871, Japan
[d] Department of Plastic Surgery, Bellland General Hospital, 500-3 Higashiyama Naka-ku, Sakai, Osaka 599-8247, Japan
[e] Department of Orthopaedic Surgery, Gifu University Graduate School of Medicine, 1-1 Yanagito, Gifu 501-1194, Japan
[f] Department of Orthopaedic Surgery, Osaka University Graduate School of Medicine, 2-2 Yamadaoka, Suita, Osaka 565-0871, Japan
[g] Japan Science and Technology Agency, CREST, Tokyo 102-0075, Japan

ARTICLE INFO

Article history:
Received 20 September 2014
Available online 8 October 2014

Keywords:
Retinoic acid
Growth plate
Cyp26b1
Chondrocytes

ABSTRACT

Retinoic acid (RA) is an active metabolite of vitamin A and plays important roles in embryonic development. CYP26 enzymes degrade RA and have specific expression patterns that produce a RA gradient, which regulates the patterning of various structures in the embryo. However, it has not been addressed whether a RA gradient also exists and functions in organs after birth. We found localized RA activities in the diaphyseal portion of the growth plate cartilage were associated with the specific expression of *Cyp26b1* in the epiphyseal portion in juvenile mice. To disturb the distribution of RA, we generated mice lacking *Cyp26b1* specifically in chondrocytes (*Cyp26b1*$^{\Delta chon}$ cKO). These mice showed reduced skeletal growth in the juvenile stage. Additionally, their growth plate cartilage showed decreased proliferation rates of proliferative chondrocytes, which was associated with a reduced height in the zone of proliferative chondrocytes, and closed focally by four weeks of age, while wild-type mouse growth plates never closed. Feeding the *Cyp26b1* cKO mice a vitamin A-deficient diet partially reversed these abnormalities of the growth plate cartilage. These results collectively suggest that Cyp26b1 in the growth plate regulates the proliferation rates of chondrocytes and is responsible for the normal function of the growth plate and growing bones in juvenile mice, probably by limiting the RA distribution in the growth plate proliferating zone.

1. Introduction

Retinoic acid (RA) is an active metabolite of vitamin A and plays important roles in embryonic development. The concentration of RA is controlled by the balance between its synthesis by retinaldehyde dehydrogenase (RALDH) and its degradation by CYP26 enzymes. CYP26s are a group of P450 enzymes that metabolize RA to inactive forms [1–3]. Both RALDH and Cyp26 have specific expression patterns and produce a RA gradient [4]. This RA gradient regulates the patterning of the anterior–posterior axis of various structures, including the hindbrain and paraxial mesoderm [5]. The RA gradient also regulates the proximodistal patterning and outgrowth of the developing limbs. *Cyp26b1* is expressed in the distal region of developing limb buds, and mice that lack *Cyp26b1* show severe limb malformation due to the spreading of the RA signal toward the distal end of the developing limb, causing abnormal patterning of limb skeletal elements [6]. However, whether this RA gradient also regulates the growth and maintenance of organs after birth has not been addressed.

The growth plate cartilage is where bone growth occurs in juveniles. Growth plate cartilage is located in the metaphysis at each end of long bones. Chondrocytes residing at the epiphyseal side in the growth plate cartilage proliferate and subsequently undergo hypertrophy just after stopping proliferation. As a result, chondrocytes change from proliferating chondrocytes on the

Abbreviations: RA, retinoic acid; *RARE*, RA-responsive elements; *Cyp26b1*$^{\Delta chon}$ cKO, *11Enh-Cre Cyp26b1*$^{flox/flox}$ conditional knockout.

* Corresponding author at: Department of Cell Growth and Differentiation, Center for iPS Cell Research and Application, Kyoto University, 53 Kawahara-cho, Shogoin, Sakyo-ku, Kyoto 606-8507, Japan. Fax: +81 75 366 7047.
E-mail address: ntsumaki@cira.kyoto-u.ac.jp (N. Tsumaki).

http://dx.doi.org/10.1016/j.bbrc.2014.10.001
0006-291X/

epiphyseal side to hypertrophic chondrocytes on the diaphyseal side of growth plate cartilage. The hypertrophic chondrocytes residing at the diaphyseal end of the growth plate cartilage subsequently die, and the hypertrophic cartilage is degraded and gradually replaced by bone. Through this mechanism, the bone becomes elongated. Thus, strict regulation of chondrocyte proliferation and hypertrophic differentiation is necessary for the normal growth of bones.

In juveniles, focal closures of the growth plate in the distal tibia [7], the proximal tibia [8], the distal tibia, elbow, proximal femur and distal femur [9] are caused by the treatment of acne with retinoids [7] or the treatment of hyperkeratinosis with cis-retinoic acid [8,9]. In guinea pigs, the application of RA caused closure of the growth plates in the proximal tibia [10]. These clinical and preclinical manifestations indicate that vitamin A and its metabolites play important roles in the bone growth of juveniles. The RA signal has been shown to regulate bone growth after birth. The deletion of RA receptors (RAR) in chondrocytes disturbs skeletal growth due to abnormal chondrocyte differentiation and disturbed matrix synthesis within the growth plates in mice [11]. Additionally, a localized distribution of RA was detected in the growth plate cartilage of the ribs of three-week-old rabbits [12]. However, it remains to be determined how RA regulates the bone growth of juveniles. In this study, we found that the expression of Cyp26b1 specifically in the proliferative chondrocyte zone was associated with localized RA activities in the zone of hypertrophic chondrocytes in the growth plate cartilage of juvenile mice. To disturb the distribution of RA, we inactivated Cyp26b1 in the growth plate using Cyp26b1 conditional knock-out mice. The resulting mouse phenotype suggests that Cyp26b1 within the growth plate regulates the proliferation rates of chondrocytes and bone growth in juveniles.

2. Materials and methods

2.1. Animals and PCR genotyping procedures

RARE-LacZ mice were a gift from Dr. Janet Rossant [13]. To generate *Cyp26b1* conditional knockout mice, *11Enh-Cre* transgenic mice [14,15] and *Cyp26b1*$^{flox/flox}$ mice [16] were prepared and mated to generate *11Enh-Cre; Cyp26b1*$^{flox/+}$ mice. Then, the *11Enh-Cre; Cyp26b1*$^{flox/+}$ and *Cyp26b1*$^{flox/flox}$ mice were intercrossed, and the *11Enh-Cre; Cyp26b1*$^{flox/flox}$ mice were considered conditional knockout (*Cyp26b1*$^{\Delta chon}$ cKO) mice. The *11Enh-Cre; Cyp26b1*$^{flox/+}$ mice were used as controls.

For genotyping, genomic DNA was isolated from the tail tips or embryonic skin and subjected to PCR analysis, according to a previously described method for the *Cre* transgene [14] and *Cyp26b1* allele [16].

2.2. Frozen sectioning and laser capture microdissection (LMD)

Mouse hindlimbs were harvested without fixation and were immediately embedded in SCEM compound (SECTION-LAB, Hiroshima, Japan). Frozen sections were prepared at 6-μm thickness with a Cryofilm type 2c(9) (SECTION-LAB) using a CM3050S cryomicrotome (Leica), according to the method described by Kawamoto [17]. The sections were briefly fixed with 100% ethanol. Semiserial sections were then stained with hematoxylin and eosin.

For LMD, frozen sections were prepared with LMD film (SECTION-LAB) using a cryomicrotome. The sections were freeze-dried in the cryostat chamber at −25 °C for one hour and briefly fixed with 100% ethanol. The proliferative zone and hypertrophic zone in the growth plate were individually captured and microdissected from cryosections using a Leica LMD7000 device (Leica) and put onto the dip of the lid of 0.5 ml tubes with cold TRIzol (Life Technologies, Tokyo, Japan).

2.3. Real-time RT-PCR

RNA was extracted from the collected samples using RNeasy Mini Kits (Qiagen, Tokyo, Japan). The total RNA was digested with DNase to eliminate any contaminating genomic DNA. For real-time quantitative RT-PCR analyses, 1 μg of total RNA was reverse-transcribed into first-strand cDNA using ReverTra Ace (Toyobo, Osaka, Japan) and random primers. The PCR amplification was performed in a reaction volume of 20 μl containing 2 μl of cDNA, 10 μl of SYBR FAST qPCR Master Mix (Kapa Biosystems, Tokyo, Japan) and 7900HT (Applied Biosystems). The RNA expression levels were normalized to the level of *Gapdh* expression. The primers used are listed in Table 1.

2.4. Staining of the skeleton

Mouse limbs were dissected, fixed in 100% ethanol overnight and then stained with Alcian blue, followed by Alizarin red S solution, according to standard protocols [18].

2.5. Histological analysis

Mouse limbs were dissected, fixed in 4% paraformaldehyde, processed and embedded in paraffin. For the immunohistochemical analysis, sections were incubated with an anti-CYP26B1 antibody (Scrum Inc., Tokyo, Japan) and an anti-type X collagen antibody (COSMO BIO CO., Ltd., Tokyo, Japan). Immune complexes were detected using secondary antibodies conjugated to Alexa Fluor 555 and Alexa Fluor 546, respectively.

2.6. BrdU staining

Mice were intraperitoneally injected with BrdU labeling reagent (10 μl/g body weight) (Zymed Laboratories Inc., South San Francisco, CA) two hours before being sacrificed. The mice were then dissected and sectioned. The incorporated BrdU was detected using a BrdU staining kit (Zymed Laboratories, Inc., South San Francisco, CA) to distinguish actively proliferating cells. The mean number of BrdU-positive cells/total cells ± standard deviation (S.D.) was calculated.

2.7. Microscope

Images were acquired on an inverted microscope (Eclipse Ti; Nikon) equipped with cameras (DS-Fi1; Nikon and C4742-80-12AG; Hamamatsu photonics) and the NIS Elements software program (Nikon).

Table 1
Primer sequences used in this study.

Primer	Sequence (5′–3′)
Col2a1 S	TTGAGACAGCACGACGTGGAG
Col2a1 AS	AGCCAGGTTGCCATCGCCATA
Col10a1 S	GGTGTGAATGGGCGGAAAG
Col10a1 AS	GCTTCCCAATACCTTCTCGTC
MMP13 S	TGTTTGCAGAGCACTACTTGAA
MMP13 AS	CAGTCACCTCTAAGCCAAAGAAA
Runx2 S	CCGCACGACAACCGCACCAT
Runx2 AS	CGCTCCGGCCCACAAATCTC
Beta galactosidase S	CTCAAACTGGCAGATGCACGGT
Beta galactosidase AS	CGTTGCACCACAGATGAAACGC
Cyp26b1 S	GCAAGATCCTACTGGGCGAAC
Cp26b1 AS	TTGGGCAGGTAGCTCTCAAGT
Gapdh S	AAGCCCATCACCATCTTCCAGGAG
Gapdh AS	ATGAGCCCTTCCACAATGCCAAAG

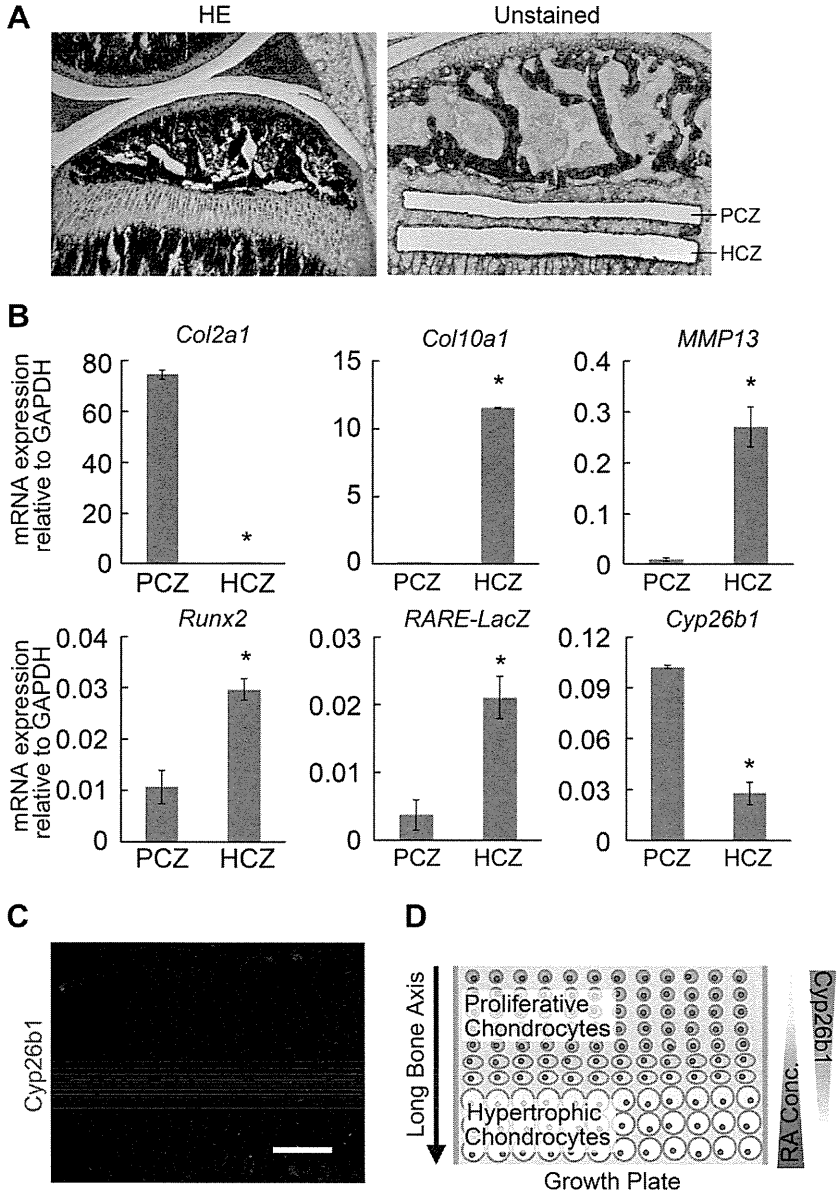

Fig. 1. Regulated RA distribution along the long axis of long bones within the growth plate cartilage. (A) We microdissected the growth plate cartilage of the proximal tibia to obtain chondrocytes from the proliferative zone (PCZ) and hypertrophic zone (HCZ) from *RARE-LacZ* mice at 2.5 weeks after birth. *Left*, a semiserial section was stained with hematoxylin and eosin. *Right*, a residual section after microdissection. (B) RNAs were extracted from cells in the proliferative chondrocyte zone (PCZ) and cells in the hypertrophic chondrocyte zone (HCZ), which were respectively obtained by microdissection, and were subjected to a real-time RT-PCR expression analysis for the genes indicated at the top of each graph. $^{*}P < 0.01$ ($n = 5$). (C) Histological sections of growth plate cartilage from the proximal tibias from three-week-old mice were immunostained with an anti-CYP26B1 antibody (Red). Bar: 100 μm. (D) A schematic representation of the RA concentration and *Cyp26b1* expression within the growth plate cartilage. Regulated RA activities were found along the long axis of the long bone within the growth plate cartilage and attributed to the localized expression of CYP26B1 in the proliferative chondrocyte zone.

2.8. Statistical analyses

Data are shown as the means and S.D. Student's *t*-test was used to compare data. *P* values <0.05 were considered statistically significant.

3. Results

3.1. Localized expression of Cyp26b1 and regulation of RA activities along the direction of bone elongation within the growth plate cartilage

To test our hypothesis that a RA gradient exists within the growth plate cartilage, we employed *RARE-lacZ* transgenic mice, in which *lacZ* is expressed under the control of RA-responsive elements (*RARE*) [13]. Because trabecular bone shows high background galactosidase activities, it is difficult to detect transgene-specific lacZ activities in bone, especially after birth. Therefore, we microdissected the growth plate cartilage, obtained cells from the proliferative chondrocyte and hypertrophic zones (Fig. 1A), and subjected them to an analysis of the expression of the *lacZ* transgene mRNA by real-time RT-PCR. The expression analysis of proliferative and hypertrophic chondrocyte markers confirmed that cells were isolated appropriately by microdissection (Fig. 1B). *LacZ* was much more highly expressed in the hypertrophic chondrocytes than in the proliferative chondrocytes (Fig. 1B). Interestingly, we detected a much higher level of *Cyp26b1* mRNA expression in the proliferative chondrocytes than in the

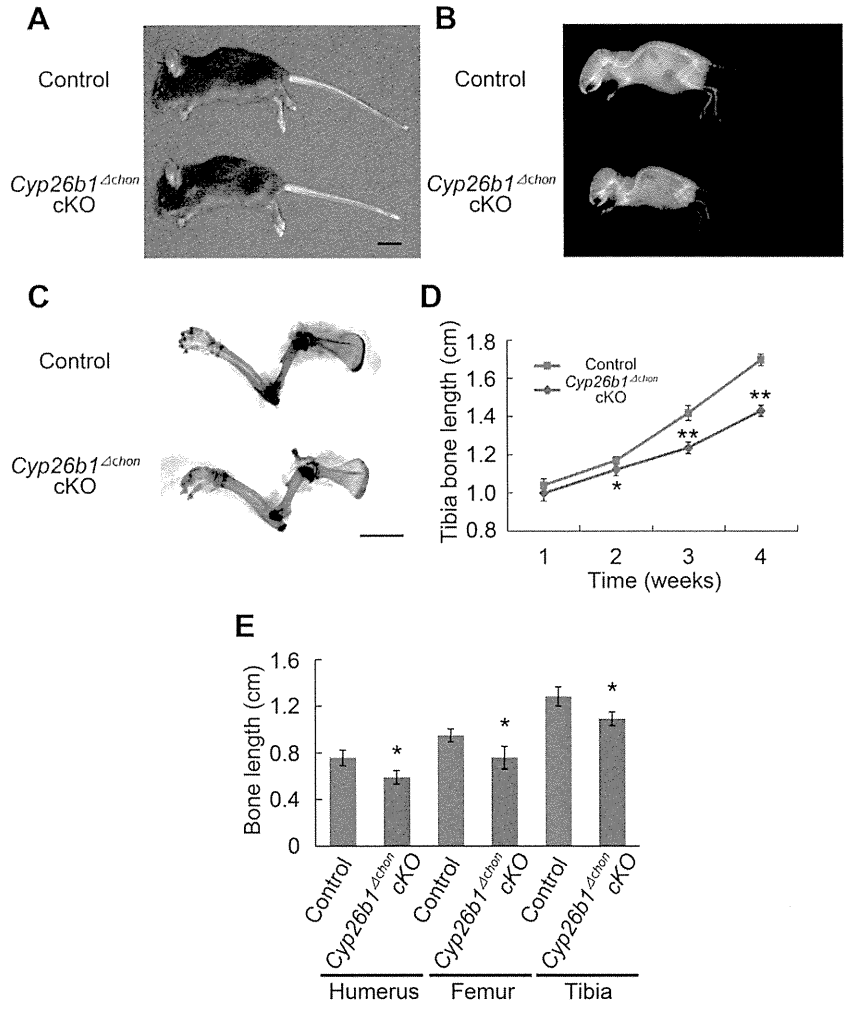

Fig. 2. The skeletal phenotype of *11Enh-Cre; Cyp26b1*$^{flox/flox}$ (*Cyp26b1*$^{\Delta chon}$) cKO mice and *11Enh-Cre; Cyp26b1*$^{flox/+}$ control mice. (A) The gross appearances of mice three weeks after birth. *Cyp26b1*$^{\Delta chon}$ cKO mice exhibited dwarfism with a short snout. Bar: 1 cm. (B) X-ray images of mice three weeks after birth. (C) The skeletons of the forelimbs of mice three weeks after birth. Alcian blue/Alizarin red staining. Bar: 5 mm. (D) The lengths of the tibiae at one, two, three and four weeks after birth. $^{*}P < 0.05$; $^{**}P < 0.01$ ($n = 5$). (E) Lengths of the humeri, femurs and tibiae three weeks after birth. $^{*}P < 0.01$ ($n = 5$).

hypertrophic chondrocytes (Fig. 1B). Accordingly, immunohistochemical analysis showed that CYP26B1 was expressed more abundantly in proliferative chondrocytes than in hypertrophic chondrocytes (Fig. 1C). These results suggest that regulated RA distribution along the direction of the bone elongation exists within the growth plate cartilage and is generated by the exclusive localization of CYP26B1 in the proliferative chondrocyte zone (Fig. 1D).

3.2. *Cyp26b1* deletion in chondrocytes disturbs the bone growth in juveniles

To disturb the distribution of RA, we deleted *Cyp26b1* in the proliferative chondrocytes of the growth plate cartilage by generating *11Enh-Cre; Cyp26b1*$^{flox/flox}$ conditional knockout (*Cyp26b1*$^{\Delta chon}$ cKO) mice. The *11Enh-Cre* transgene directed Cre expression in the proliferative chondrocytes after the completion of skeletal patterning under the control of the promoter/enhancer sequence of the type XI collagen α2 chain gene (*Col11a2*) [14,15]. *Cyp26b1*$^{\Delta chon}$ cKO mice showed normal skeletal patterning, skeletal development and bone length until one week after birth. However, at three weeks after birth, they started to show a chondrodysplasia phenotype that included dwarfism and a short snout (Fig. 2A and B). A precise examination of the lengths of skeletal elements revealed a gradual decrease in the lengths of bones compared to control mice beginning from two weeks after birth (Fig. 2C–E), and all long bones in the *Cyp26b1*$^{\Delta chon}$ cKO mice were shorter than those in the controls at three weeks after birth.

To analyze the mechanism responsible for the shorter bones in the *Cyp26b1*$^{\Delta chon}$ cKO mice, we performed a histological analysis of their growth plates. We noticed a slight decrease in the height of the proliferative chondrocyte zone at two weeks after birth (Fig. 3A, top row). The height of the proliferative chondrocyte zone was significantly decreased at three weeks after birth, especially at the central portion (Fig. 3A, middle row, and Fig. 3B). Immunohistochemistry using an anti-type X collagen antibody revealed that the location of the hypertrophic cartilage zone that produced type X collagen was shifted toward the epiphysis in Cyp26b1 cKO mice, clarifying the decreased height of the zone of proliferative chondrocytes (Fig. 3C) to the central portion.

The growth plate was closed at the central portion at four weeks after birth (Fig. 3A, bottom row), and growth plate closure was recognized in all bones examined, including the tibia, humerus and femur (Fig. 3A and D). BrdU labeling analysis revealed significantly decreased proliferation rates of the proliferative chondrocytes when the mice were one and three weeks old (Fig. 4A–C). These results suggest that the decreased proliferation rates of the

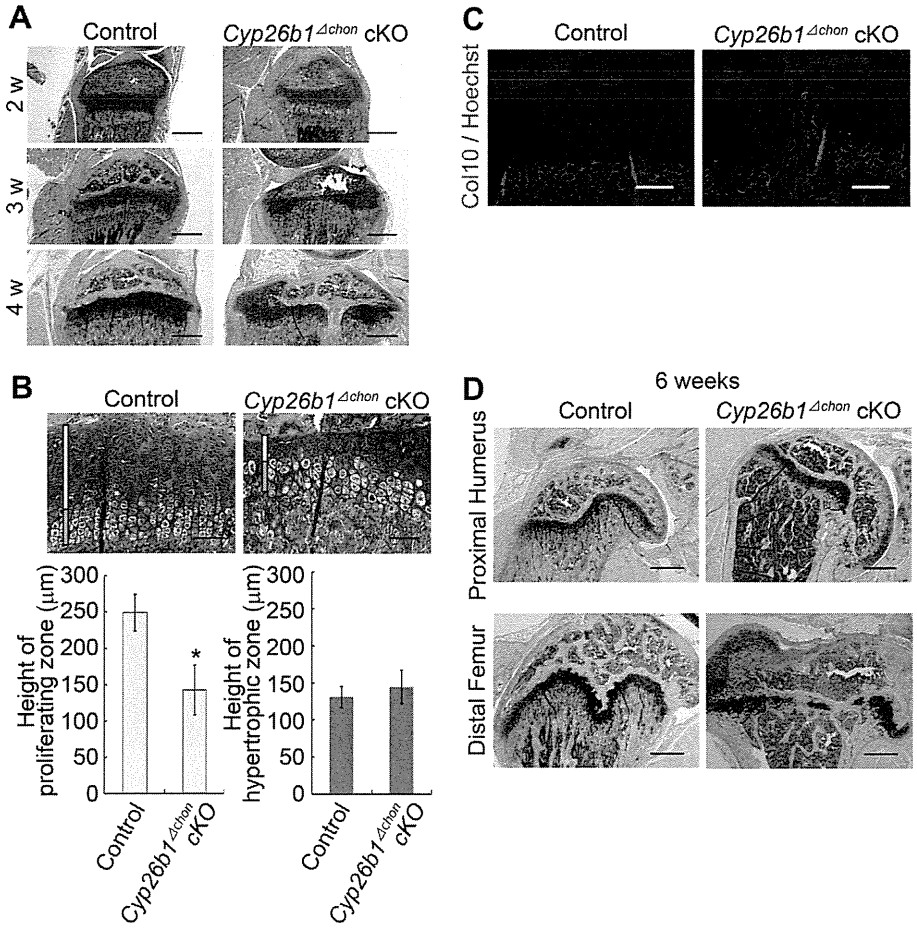

Fig. 3. Histological analysis of the growth plate cartilage of *Cyp26b1*$^{\Delta chon}$ cKO mice. (A) Sagittal sections of the proximal tibia at two, three and four weeks after birth. Safranin O-fast green-iron hematoxylin staining. Bar: 500 μm. (B) *Top*, Magnified image of the central part of the growth plate cartilage in the proximal tibia three weeks after birth. Safranin O-fast green-iron hematoxylin staining. Yellow bars indicate the height of the proliferative chondrocyte zone. Blue bars denote the height of the hypertrophic chondrocyte zone. Bars: 100 μm. Bottom, the mean ± S.D. of the height of the proliferative chondrocyte zone (left) and the hypertrophic chondrocyte zone (right). *$P < 0.01$ ($n = 5$). (C) Sagittal sections of the proximal tibia at three weeks after birth were immunostained with an anti-type X collagen antibody. Bars: 100 μm. (D) Histology of the growth plate cartilage in the proximal humerus and distal femur in *Cyp26b1*$^{\Delta chon}$ cKO mice six weeks after birth. Safranin O-fast green-iron hematoxylin. Bars: 500 μm.

proliferative chondrocytes can explain the decreased heights of the proliferative chondrocyte zone, the subsequent closure of the growth plates and the suppression of bone growth.

3.3. Reversion of the growth plate abnormalities by feeding *Cyp26b1*$^{\Delta chon}$ cKO mice a vitamin A-deficient diet

The immunohistochemical analysis confirmed that CYP26B1 was absent in the proliferative chondrocytes of *Cyp26b1*$^{\Delta chon}$ cKO mice (Fig. 4D), and that this absence could cause a disturbance in the RA distribution within the growth plate.

To confirm that the elevated concentration of RA in the proliferative chondrocytes of *Cyp26b1*$^{\Delta chon}$ cKO mice was responsible for the decreased proliferation rates, we fed the mice a vitamin A-deficient diet which systemically decreased RA concentrations [19]. Following this diet, *Cyp26b1*$^{\Delta chon}$ cKO mice showed a partial reversion in the decreased proliferation rates of the proliferative chondrocytes (Fig. 4E) and corresponding partial reversion in the decreased height of the proliferative chondrocyte zone (Fig. 4F). These results collectively suggest that the distribution of RA, which is generated by the proliferative chondrocyte-specific expression of *Cyp26b1*, regulates the proliferation rates of chondrocytes and subsequently controls the growth rates and closure of growth plates to determine the length of bones in juveniles.

4. Discussion

It is well known that the RA gradient regulates the patterning of spatial structures in mammals during development. Cyp26b1 is a critical regulator of the distribution of RA, and Cyp26b1 KO and cKO studies have demonstrated that Cyp26b1 deletion alters the RA distribution in various tissues [5,16,20,21]. The present study provides evidence that Cyp26b1 within the growth plate cartilage is important for normal chondrocyte proliferation/differentiation and bone growth in juvenile mice, probably through its regulation of the RA distribution in the growth plate.

We detected localized RA activities within the growth plate cartilage in juvenile mice, as indicated by the increased *RARE-lacZ* expression toward hypertrophic chondrocytes (Fig. 1B). The existence of a possible RA gradient within the growth plate is supported by a previous report demonstrating that the RA content measured by MS quantification was lower in the resting and proliferative chondrocyte zone than that in the hypertrophic chondrocyte zone in the growth plate cartilage of the ribs of three-week old rabbits [12]. It was reported that *RARE-lacZ* expression is not

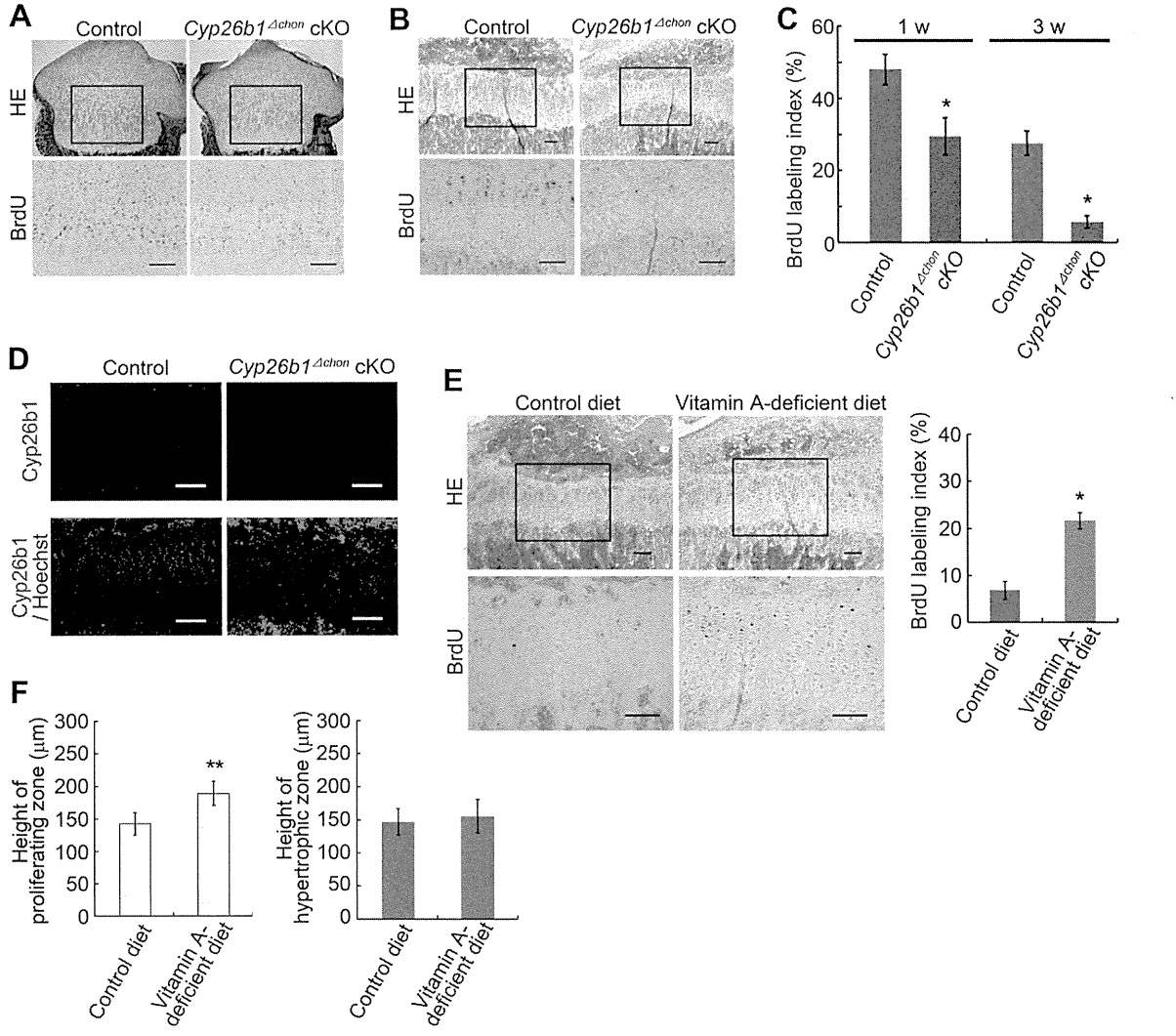

Fig. 4. Proliferation rates and Cyp26b1 expression of chondrocytes in the growth plate cartilage, and the effects of a vitamin A-deficient diet on the growth plate cartilage in the proximal tibias of *Cyp26b1*$^{\Delta chon}$ cKO mice. (A, B, C) BrdU was injected intraperitoneally into the mice two hours before sacrifice. One-week old mice (A) and three-week old mice (B). Top, hematoxylin–eosin staining. Bottom, semiserial sections were immunostained with an anti-BrdU antibody. Regions corresponding to the boxed regions in the top are magnified and shown. Bars: 100 μm. (C) Ratios (%) of the number of BrdU-positive cells to the numbers of total cells in the proliferative chondrocyte zone. *$P < 0.01$ ($n = 5$). (D) Histological sections of the growth plate cartilage in the proximal tibias of three-week-old mice were immunostained with an anti-Cyp26b1 antibody (Red). The blue color is Hoechst stain, which indicates nuclei. Bars: 100 μm. (E, F) Effects of a vitamin A-deficient diet on the growth plate cartilage of *Cyp26b1*$^{\Delta chon}$ cKO mice. The mothers of *Cyp26b1*$^{\Delta chon}$ cKO pups were fed with a vitamin A-deficient diet or a control diet from eight weeks before gestation until the sacrifice of the *Cyp26b1*$^{\Delta chon}$ cKO pups three weeks after birth. The pups consumed either their mother's milk or shared an identical diet with their mother. (E) *Left*, BrdU was injected intraperitoneally into the mice two hours before sacrifice. Top, hematoxylin–eosin staining. Bottom, semiserial sections were immunostained with an anti-BrdU antibody. Regions corresponding to the boxed regions in the top are magnified and shown. Bars: 100 μm. *Right*, ratios (%) of the number of BrdU-positive cells to the number of total cells in the proliferative chondrocyte zone. *$P < 0.01$ ($n = 5$). (F) Mean ± S.D. of the height of the proliferative chondrocyte zone (left) and the hypertrophic chondrocyte zone (right). **$P < 0.05$ ($n = 5$).

detectable or is limited in the primordial cartilage during the embryonic stage [22], which is consistent with the normal embryonic development of *Cyp26b1*$^{\Delta chon}$ cKO mice in this study.

The partial recovery of growth plate abnormalities in *Cyp26b1*$^{\Delta chon}$ cKO mice by a vitamin A-deficient diet supports the notion that *Cyp26b1* deletion caused abnormalities through elevated RA activities in the growth plate. Accordingly, the decreased proliferation rates of proliferative chondrocytes in *Cyp26b1*$^{\Delta chon}$ cKO mice suggest that excess RA inhibits the proliferation of proliferative chondrocytes. Previous studies on the effects of RA have yielded conflicting data regarding its regulation of the differentiation of chondrocytes in the growth plate [23]. Ballock et al. reported that RA blocks the stimulatory effects of thyroid hormone on cultured rat chondrocyte hypertrophy [23], whereas others showed RA induces the hypertrophy of cultured chick chondrocytes [24,25]. Such in vitro culture experiments are affected by the pharmacological dosage of RA, variations in the species, culture conditions, composition of serum and the anatomical source of the growth plate cells used [23]. Our in vivo results are less susceptible to the above problems to better clarify the function of RA in chondrocyte proliferation/differentiation in the growth plate and in the bone growth.

Excess intake of vitamin A causes growth impairment and skeletal pain in juveniles [7–9]. Our study provides evidence that regulation of the RA distribution occurs within the growth plate cartilage and that this regulation plays critical roles in controlling the growth of long bones in juvenile mice. Our results also show that exogenous vitamin A can affect this regulation and distribution, since a vitamin A-deficient diet partially rescued the growth plate structure of *Cyp26b1*$^{\Delta chon}$ cKO mice. The characteristics of the closure of the growth plate seen in a child receiving excess RA [8] and guinea pigs receiving a RAR agonist [10] were similar

to those seen in *Cyp26b1*$^{\Delta chon}$ cKO mice in that the closure occurred in the central part of the growth plate, suggesting that a similar form of regulation occurs in humans and mice.

Acknowledgments

We thank Hiroshi Hamada and Satoru Mamiya for the *Cyp26b1* flox mice, Aki Takimoto, Chisa Shukunami and Yuji Hiraki for instructions about the cryostat sectioning, Janet Rossant for the RARE-LacZ mice, Peter Karagiannis for reading the manuscript, and Hiromi Kishi, Minoru Okada, Akihiro Yamashita and Miho Morioka for assistance and helpful discussions. This study was supported in part by the Japan Science Technology Agency (JST), CREST (to N.T.), Scientific Research Grant No. 23792042 (to Y. M.) and No. 24390354 (to N.T.) from MEXT.

References

[1] H. Fujii, T. Sato, S. Kaneko, O. Gotoh, Y. Fujii-Kuriyama, K. Osawa, S. Kato, H. Hamada, Metabolic inactivation of retinoic acid by a novel P450 differentially expressed in developing mouse embryos, EMBO J. 16 (1997) 4163–4173.

[2] W.J. Ray, G. Bain, M. Yao, D.I. Gottlieb, CYP26, a novel mammalian cytochrome P450, is induced by retinoic acid and defines a new family, J. Biol. Chem. 272 (1997) 18702–18708.

[3] J.A. White, Y.D. Guo, K. Baetz, B. Beckett-Jones, J. Bonasoro, K.E. Hsu, F.J. Dilworth, G. Jones, M. Petkovich, Identification of the retinoic acid-inducible all-trans-retinoic acid 4-hydroxylase, J. Biol. Chem. 271 (1996) 29922–29927.

[4] S. Shimozono, T. Iimura, T. Kitaguchi, S. Higashijima, A. Miyawaki, Visualization of an endogenous retinoic acid gradient across embryonic development, Nature 496 (2013) 363–366.

[5] Y. Sakai, C. Meno, H. Fujii, J. Nishino, H. Shiratori, Y. Saijoh, J. Rossant, H. Hamada, The retinoic acid-inactivating enzyme CYP26 is essential for establishing an uneven distribution of retinoic acid along the anterio-posterior axis within the mouse embryo, Genes Dev. 15 (2001) 213–225.

[6] K. Yashiro, X. Zhao, M. Uehara, K. Yamashita, M. Nishijima, J. Nishino, Y. Saijoh, Y. Sakai, H. Hamada, Regulation of retinoic acid distribution is required for proximodistal patterning and outgrowth of the developing mouse limb, Dev. Cell 6 (2004) 411–422.

[7] F. Luthi, Y. Eggel, N. Theumann, Premature epiphyseal closure in an adolescent treated by retinoids for acne: an unusual cause of anterior knee pain, Joint Bone Spine 79 (2012) 314–316.

[8] L.M. Milstone, J. McGuire, R.C. Ablow, Premature epiphyseal closure in a child receiving oral 13-cis-retinoic acid, J. Am. Acad. Dermatol. 7 (1982) 663–666.

[9] J. Prendiville, E.A. Bingham, D. Burrows, Premature epiphyseal closure – a complication of etretinate therapy in children, J. Am. Acad. Dermatol. 15 (1986) 1259–1262.

[10] A.M. Standeven, P.J. Davies, R.A. Chandraratna, D.R. Mader, A.T. Johnson, V.A. Thomazy, Retinoid-induced epiphyseal plate closure in guinea pigs, Fundam. Appl. Toxicol. 34 (1996) 91–98.

[11] J.A. Williams, N. Kondo, T. Okabe, N. Takeshita, D.M. Pilchak, E. Koyama, T. Ochiai, D. Jensen, M.-L. Chu, M.A. Kane, J.L. Napoli, M. Enomoto-Iwamoto, N. Ghyselinck, P. Chambon, M. Pacifici, M. Iwamoto, Retinoic acid receptors are required for skeletal growth, matrix homeostasis and growth plate function in postnatal mouse, Dev. Biol. 328 (2009) 315–327.

[12] J.A. Williams, M. Kane, T. Okabe, M. Enomoto-Iwamoto, J.L. Napoli, M. Pacifici, M. Iwamoto, Endogenous retinoids in mammalian growth plate cartilage: analysis and roles in matrix homeostasis and turnover, J. Biol. Chem. 285 (2010) 36674–36681.

[13] J. Rossant, R. Zirngibl, D. Cado, M. Shago, V. Giguere, Expression of a retinoic acid response element-hsplacZ transgene defines specific domains of transcriptional activity during mouse embryogenesis, Genes Dev. 5 (1991) 1333–1344.

[14] T. Iwai, J. Murai, H. Yoshikawa, N. Tsumaki, Smad7 inhibits chondrocyte differentiation at multiple steps during endochondral bone formation and down-regulates p38 MAPK pathways, J. Biol. Chem. 283 (2008) 27154–27164.

[15] D. Ikegami, H. Akiyama, A. Suzuki, T. Nakamura, T. Nakano, H. Yoshikawa, N. Tsumaki, Sox9 sustains chondrocyte survival and hypertrophy in part through Pik3ca-Akt pathways, Development 138 (2011) 1507–1519.

[16] J. Okano, U. Lichti, S. Mamiya, M. Aronova, G. Zhang, S.H. Yuspa, H. Hamada, Y. Sakai, M.I. Morasso, Increased retinoic acid levels through ablation of Cyp26b1 determine the processes of embryonic skin barrier formation and peridermal development, J. Cell Sci. 125 (2012) 1827–1836.

[17] T. Kawamoto, Use of a new adhesive film for the preparation of multi-purpose fresh-frozen sections from hard tissues, whole-animals, insects and plants, Arch. Histol. Cytol. 66 (2003) 123–143.

[18] P.W.J. Peters, Double staining of fetal skeletons for cartilage and bone, in: H.J.M.D. Neuberg, T.E. Kwasigroch (Eds.), Methods in Prenatal Toxicology, Georg Thieme Verlag, Stuttgart, Germany, 1977, pp. 153–154.

[19] A.K. Verma, A. Shoemaker, R. Simsiman, M. Denning, R.D. Zachman, Expression of retinoic acid nuclear receptors and tissue transglutaminase is altered in various tissues of rats fed a vitamin A-deficient diet, J. Nutr. 122 (1992) 2144–2152.

[20] H.J. Dranse, A.V. Sampaio, M. Petkovich, T.M. Underhill, Genetic deletion of Cyp26b1 negatively impacts limb skeletogenesis by inhibiting chondrogenesis, J. Cell Sci. 124 (2011) 2723–2734.

[21] G. MacLean, H. Li, D. Metzger, P. Chambon, M. Petkovich, Apoptotic extinction of germ cells in testes of Cyp26b1 knockout mice, Endocrinology 148 (2007) 4560–4567.

[22] H.P. von Schroeder, J.N. Heersche, Retinoic acid responsiveness of cells and tissues in developing fetal limbs evaluated in a RAREhsplacZ transgenic mouse model, J. Orthop. Res. 16 (1998) 355–364.

[23] R.T. Ballock, X. Zhou, L.M. Mink, D.H. Chen, B.C. Mita, Both retinoic acid and 1,25(OH)2 vitamin D3 inhibit thyroid hormone-induced terminal differentiation of growth plate chondrocytes, J. Orthop. Res. 19 (2001) 43–49.

[24] M. Iwamoto, I.M. Shapiro, K. Yagami, A.L. Boskey, P.S. Leboy, S.L. Adams, M. Pacifici, Retinoic acid induces rapid mineralization and expression of mineralization-related genes in chondrocytes, Exp. Cell Res. 207 (1993) 413–420.

[25] M. Pacifici, E.B. Golden, M. Iwamoto, S.L. Adams, Retinoic acid treatment induces type X collagen gene expression in cultured chick chondrocytes, Exp. Cell Res. 195 (1991) 38–46.

J Bone Miner Metab (2014) 32:378–392
DOI 10.1007/s00774-013-0514-1

ORIGINAL ARTICLE

IL-6 negatively regulates osteoblast differentiation through the SHP2/MEK2 and SHP2/Akt2 pathways in vitro

Shoichi Kaneshiro · Kosuke Ebina · Kenrin Shi · Chikahisa Higuchi · Makoto Hirao · Michio Okamoto · Kota Koizumi · Tokimitsu Morimoto · Hideki Yoshikawa · Jun Hashimoto

Received: 13 February 2013 / Accepted: 7 August 2013 / Published online: 12 October 2013

Abstract It has been suggested that interleukin-6 (IL-6) plays a key role in the pathogenesis of rheumatoid arthritis (RA), including osteoporosis not only in inflamed joints but also in the whole body. However, previous in vitro studies regarding the effects of IL-6 on osteoblast differentiation are inconsistent. The aim of this study was to examine the effects and signal transduction of IL-6 on osteoblast differentiation in MC3T3-E1 cells and primary murine calvarial osteoblasts. IL-6 and its soluble receptor significantly reduced alkaline phosphatase (ALP) activity, the expression of osteoblastic genes (Runx2, osterix, and osteocalcin), and mineralization in a dose-dependent manner, which indicates negative effects of IL-6 on osteoblast differentiation. Signal transduction studies demonstrated that IL-6 activated not only two major signaling pathways, SHP2/MEK/ERK and JAK/STAT3, but also the SHP2/PI3K/Akt2 signaling pathway. The negative effect of IL-6 on osteoblast differentiation was restored by inhibition of MEK as well as PI3K, while it was enhanced by inhibition of STAT3. Knockdown of MEK2 and Akt2 transfected with siRNA enhanced ALP activity and gene expression of Runx2. These results indicate that IL-6 negatively regulates osteoblast differentiation through SHP2/MEK2/ERK and SHP2/PI3K/Akt2 pathways, while affecting it positively through JAK/STAT3. Inhibition of MEK2 and Akt2 signaling in osteoblasts might be of potential use in the treatment of osteoporosis in RA.

Keywords Interleukin-6 · Osteoblast differentiation · MEK2 · Akt2 · Signaling pathway

Introduction

Inflammation-mediated bone loss is a major feature of various bone diseases, including rheumatoid arthritis (RA). Interleukin-6 (IL-6) contributes to the development of arthritis and is present at high concentrations in the serum and synovial fluid of patients with RA [1–4]. Soluble IL-6 receptor (sIL-6R) is also elevated in the serum and synovial fluid of RA patients [5, 6], and IL-6 exerts its action by binding either to its membrane-bound receptor (mIL-6R) or to sIL-6R. Moreover, IL-6 is closely associated with the expression of receptor activator of NF-κB ligand (RANKL) in osteoblasts [7]. That is to say, IL-6 acts indirectly on osteoclastogenesis by stimulating the release of RANKL by cells within bone tissues such as osteoblasts [8]. It can unquestionably be said that IL-6 plays a major role in the pathogenesis of RA [9–12], including osteoporosis not only in inflamed joints but also in the whole body.

There have been several studies on the effect of IL-6 on bone turnover in animal models. In IL-6 knock-out mice,

Electronic supplementary material The online version of this article (doi:10.1007/s00774-013-0514-1) contains supplementary material, which is available to authorized users.

S. Kaneshiro · K. Ebina (✉) · K. Shi · C. Higuchi · M. Okamoto · K. Koizumi · T. Morimoto · H. Yoshikawa
Department of Orthopaedic Surgery, Graduate School of Medicine, Osaka University, 2-2 Yamadaoka, Suita, Osaka 565-0871, Japan
e-mail: k-ebina@umin.ac.jp

M. Hirao
Department of Orthopaedic Surgery, Osaka Minami Medical Center, National Hospital Organization, 2-1 Kidohigashi, Kawachinagano, Osaka 586-8521, Japan

J. Hashimoto
Department of Rheumatology, Osaka Minami Medical Center, National Hospital Organization, 2-1 Kidohigashi, Kawachinagano, Osaka 586-8521, Japan